

COMMISSARIAT A L'ENERGIE ATOMIQUE

CENTRE D'ETUDES NUCLEAIRES DE SACLAY

Service de Documentation

F91191 GIF SUR YVETTE CEDEX

CEA-CONF-- 8955

L1

GAIA : A 2-D CURVILINEAR MOVING GRID HYDRODYNAMIC CODE

Jourdren, H.

CEA Centre d'Etudes de Limeil-Valenton, 94-
Villeneuve-Saint-Georges (France)

Communication présentée à :

Congress on numerical analysis
Los Alamos, NM (USA)
2-7 Feb 1987

H. JOURDREN

Centre d'Etudes de LIMEIL-VALENTON
 BP N° 27 - 94190 VILLENEUVE SAINT GEORGES
 FRANCE

INTRODUCTION

The GAIA computer code is developed for time dependent, compressible, multimaterial fluid flow problems, to overcome some drawbacks of traditional 2-D Lagrangian codes. The initial goals of robustness, entropy accuracies, efficiency in presence of large interfacial slip, have already been achieved.

The general GODUNOV approach is applied to an arbitrary time varying control-volume formulation. We review in this paper the Riemann solver, the GODUNOV cartesian and curvilinear moving grid schemes and an efficient grid generation algorithm. We finally outline a possible second order accuracy extension.

1. - AN ITERATIVE RIEMANN SOLVER

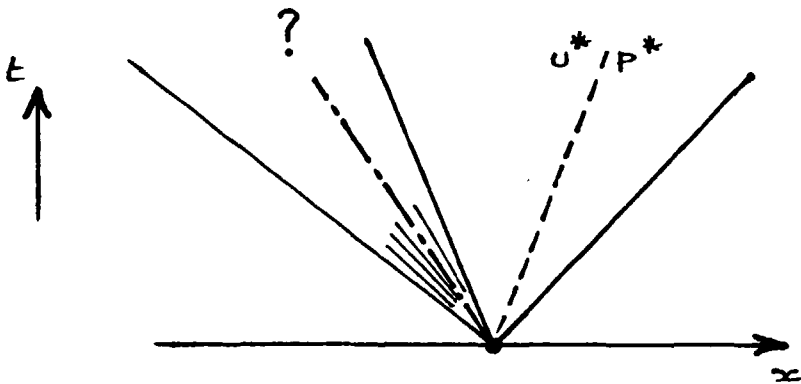
Widespread usage of the Godunov schemes in hydrodynamics has been limited by the cost and the complexity of the Riemann problem. It appeared recently that approximate solutions may be used with equal success.

1.1. Approximate relationship : $U_s = C_o + s U_p$

Dukowitz's simple and efficient Riemann solver /9/ relies on the two-shock approximation and the experimental relationship $U_s = C_o + s U_p$ relating the shock velocity to the corresponding change of fluid velocity. This solver provides the pressure P^* and the fluid velocity U^* at the contact discontinuity of the Riemann solution. It is consequently well suited for lagrangian schemes.

1.2. Simplified equation of state

Considering a Godunov moving grid scheme, the complete Riemann solution is necessary to get the hydrodynamic state "seen" by a grid point moving at an arbitrary velocity. This requires a complete equation of state.



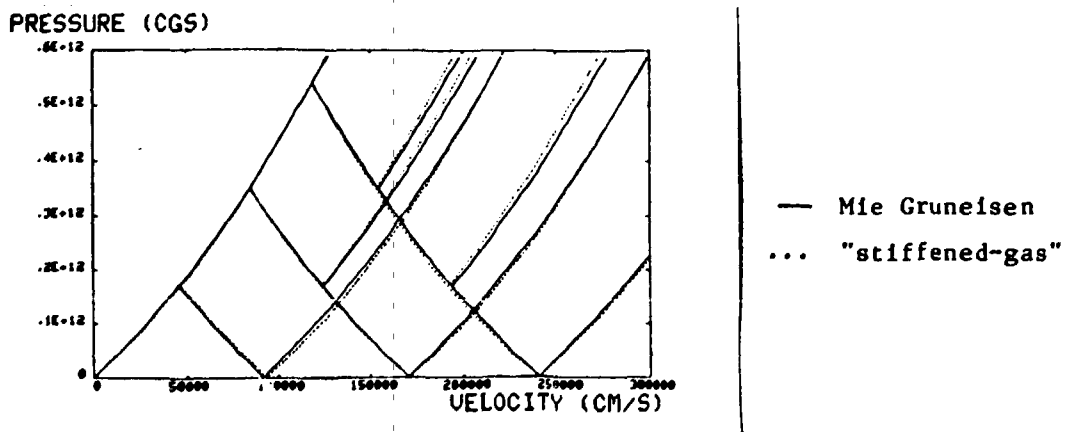
The Riemann solver used in the GAIA code operates on the "stiffened-gas" equation of state (Harlow, Amsden /4/)

$$(1) \quad P = c_0^2 (\rho - \rho_0) + (\gamma - 1) \rho \epsilon \quad (1)$$

where P is the pressure, ρ is the density and ϵ is the internal energy per unity of mass.

The form $\epsilon(P, \rho) = \frac{P + \gamma P_0}{(\gamma - 1)\rho}$ is equivalent to (1) where $P_0 = \frac{1}{\gamma} \rho_0 c_0^2$ is the spall pressure and γ the polytropic coefficient. The corresponding Riemann solver algorithm is iterative as in the case of perfect gas, but quite affordable when used in traditional hydrodynamic computations.

Remark : The "stiffened-gas" equation of state is a zeroth order development of the Gruneisen equation of state constructed on the approximate Hugoniot $U_s = C_0 + sU_p$. It constitutes a good approximation for solids, as illustrated for iron by the following shock-release diagram.



1.3 Extension to mixtures

A specific solver is required for cells containing several materials. An extended form of the "stiffened-gas" equation of state has been designed for that

purpose by A. Bourgeade, B. Scheurer and the author.

Considering two species A and B with their respective equation of state

$$\varepsilon_A(P, \rho) = \frac{P + \gamma^A P_o}{(\gamma^A - 1)\rho}, \quad \varepsilon_B(P, \rho) = \frac{P + \gamma^B P_o}{(\gamma^B - 1)\rho}$$

introducing λ the mass fraction of A, an equation for the mixture of the two species can be stated as

$$\varepsilon(P, \rho, \lambda) = \lambda \varepsilon_A(P, \rho) + (1-\lambda) \varepsilon_B(P, \rho)$$

The equivalent "stiffened-gas" formulation is :

$$(2) \quad \varepsilon(P, \rho, \lambda) = \frac{P + \Gamma(\lambda) P_o(\lambda)}{(\Gamma(\lambda) - 1)\rho}$$

$$\text{with } \Gamma(\lambda) = 1 + \frac{(\gamma^A - 1)(\gamma^B - 1)}{(1-\lambda)(\gamma^A - 1) + \lambda(\gamma^B - 1)}, \quad P_o(\lambda) = \frac{\Gamma(\lambda) - 1}{\Gamma(\lambda)} \left((1-\lambda) \frac{\gamma^B P_o^B}{\gamma^B - 1} + \lambda \frac{\gamma^A P_o^A}{\gamma^A - 1} \right)$$

2. - 2-D MOVING GRID GODUNOV'S SCHEMES

In the algorithms /1/ and /6/, convective and non convective fluxes are computed simultaneously using the complete Riemann solver solution. Then it is not necessary to decompose the scheme in a lagrangian phase and a remaping phase. The general methodology is summarized here.

2.1. Cartesian scheme

The unsteady two-dimensionnal Euler equations :

$$\frac{\partial U}{\partial t} + \frac{\partial}{\partial x} F(U) + \frac{\partial}{\partial y} G(U) = 0$$

$$\text{where : } U = \begin{pmatrix} \rho \\ \rho u \\ \rho v \\ \rho e \end{pmatrix} \quad F(U) = \begin{pmatrix} \rho u \\ \rho u^2 + p \\ \rho uv \\ (\rho e + p)u \end{pmatrix} \quad G(U) = \begin{pmatrix} \rho v \\ \rho uv \\ \rho v^2 + p \\ (\rho e + p)v \end{pmatrix}$$

can be written in integral form using the divergence theorem

$$\iint U dx dy + F dy dt + G dt dx = 0$$

An application of this formula to the closed surface (1', 2', 3', 4', 1'', 2'', 3'', 4'') delimited by the four vertices of an arbitrary moving cell during a time step Δt leads to

$$(3) \quad U^{\circ} \Omega^{\circ} = U_0 \Omega_0 + Q_{12} + Q_{23} + Q_{34} + Q_{41}$$

relating the unknowns U° at time Δt to four numerical fluxes and the corresponding known quantities U_0 at the initial time.

Using the following notations :

$$\Omega^{\circ} = \iint dx dy \quad \Omega_0 = \iint dx dy$$

(1'', 2'', 3'', 4'') (1', 2', 3', 4')

$$\Omega_{1j} = \iint_{1j} dx dy \quad ; \quad \Phi_{1j} = \iint_{1j} dy dt \quad ; \quad \Psi_{1j} = \iint_{1j} dt dx$$

the expression of a numerical flux is :

$$Q_{1j} = U_{1j} \Omega_{1j} + F_{1j} \Phi_{1j} + G_{1j} \Psi_{1j}$$

Defining average positions of vertices over the time step Δt

$$x_1 = \frac{1}{2} (x_1' + x_1'') \quad , \quad y_1 = \frac{1}{2} (y_1' + y_1'')$$

the area appearing in the numerical flux Q_{1j} are approximated by

$$\Phi_{1j} = \Delta t (y_j - y_1)$$

$$\Psi_{1j} = \Delta t (x_1 - x_j)$$

$$\Omega_{1j} = \frac{1}{2} [(x_j'' - x_1')(y_1'' - y_j') - (x_1'' - x_j')(y_j'' - y_1')]$$

Introducing a moving grid velocity W_{1j}^* that satisfies

$$Q_{1j} = \Delta t \lambda_{1j} W_{1j}^* \quad \text{with} \quad \lambda_{1j} = [(x_j - x_1)^2 + (y_j - y_1)^2]^{\frac{1}{2}}$$

the numerical flux becomes

$$Q_{1j} = U_{1j} \Delta t \lambda_{1j} W_{1j}^* + F_{1j} \Delta t (y_j - y_1) - G_{1j} \Delta t (x_j - x_1)$$

or, using direction cosines

$$\alpha_{1j} = -(y_j - y_1) / \lambda_{1j} \quad , \quad \beta_{1j} = (x_j - x_1) / \lambda_{1j}$$

$$Q_{ij} = \Delta t \ell_{ij} (U_{ij} W_{ij}^* - F_{ij} \alpha_{ij} - G_{ij} \beta_{ij})$$

An extended form is

$$(4) \quad Q_{ij} = \Delta t \ell_{ij} \begin{pmatrix} R & (W_{ij}^* - N) \\ RU & (W_{ij}^* - N) - \alpha P \\ RV & (W_{ij}^* - N) - \beta P \\ RE & (W_{ij}^* - N) - NP \end{pmatrix}_{ij} \quad (4)$$

$$\text{with } N_{ij} = \alpha_{ij} U_{ij} + \beta_{ij} V_{ij}$$

Such an expression could have been written directly. The precise derivation has been detailed for use in the more complex curvilinear case. The parameters appearing at the edges of a cell denoted with capital letters $(R, U, V, P, E)_{ij}$ are obtained by the resolution of one dimensional problems in the direction normal to the cell edge with left and right states given by these at the centers of the adjacent cells.

The density, pressure and normal component of velocity $(R, P, N)_{ij}$ "seen" by a cell edge during its displacement at velocity W_{ij}^* is extracted from the self-similar Riemann solution.

The tangential component of velocity is obtained by the comparison of the grid velocity to the contact discontinuity velocity

$$T_{ij} = \begin{cases} T_{ij}^L, & \text{if } w_{ij}^* < U^* \\ T_{ij}^R, & \text{if } w_{ij}^* > U^* \end{cases}$$

giving the cartesian components of velocity necessary in (4)

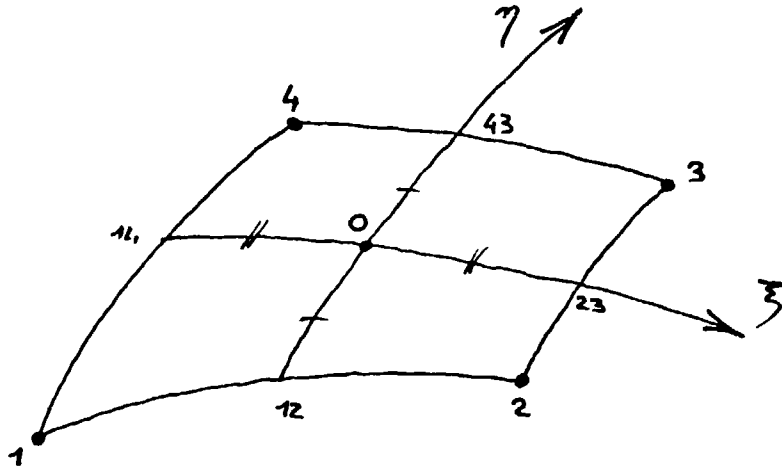
$$(5) \quad U_{ij} = N_{ij} \alpha_{ij} + T_{ij} \beta_{ij}, \quad V_{ij} = N_{ij} \beta_{ij} - T_{ij} \alpha_{ij}$$

This completes the general description of the cartesian scheme.

2.2. Curvilinear scheme

a) Local curvilinear coordinate system

A local curvilinear coordinate system is defined for each cell delimited by its four vertices (1, 2, 3, 4) at the initial time.



The following notations hold for the rest of the paper :

- direction cosines

$$\alpha' = \frac{1}{\sqrt{g_{11}}} \frac{\partial x}{\partial \xi} \quad , \quad \beta' = \frac{1}{\sqrt{g_{11}}} \frac{\partial y}{\partial \xi}$$

$$\alpha'' = \frac{1}{\sqrt{g_{22}}} \frac{\partial x}{\partial \eta} \quad , \quad \beta'' = \frac{1}{\sqrt{g_{22}}} \frac{\partial y}{\partial \eta}$$

- angle between coordinate lines

$$\alpha = \cos (\xi, \eta) = \alpha' \alpha'' + \beta' \beta''$$

$$\beta = \sin (\xi, \eta) = \alpha' \alpha'' - \beta' \beta''$$

- velocity components

. cartesian : u, v

. contravariant : $\mu = \frac{1}{\beta} (u \beta'' - v \alpha'')$, $v = \frac{1}{\beta} (v \alpha' - u \beta')$

. "intrinsic" : $\mu^k = u \alpha' + v \beta'$, $v^k = u \alpha'' + v \beta''$

$$v^n = v \alpha' - u \beta' \quad , \quad \mu^n = u \beta'' - v \alpha''$$

b) (μ^k, v^k) Euler equations

From the unsteady two-dimensional Euler equations in plane or axisymetric geometry

$$(6) \quad \frac{\partial [Q(y)\rho u]}{\partial t} + \frac{\partial [Q(y)(\rho u^2 + p)]}{\partial x} + \frac{\partial [Q(y)\rho u v]}{\partial y} = 0$$

$$(7) \quad \frac{\partial [Q(y)\rho v]}{\partial t} + \frac{\partial [Q(y)\rho u v]}{\partial x} + \frac{\partial [Q(y)(\rho v^2 + p)]}{\partial y} = -p \frac{dQ}{dy}$$

with $Q(y) = 1, y$

one can derive evolution equations for the tangential velocity component to each co-ordinate line.

$$\begin{aligned} \alpha'(6) + \beta'(7) \quad & \frac{\partial [Q(y)\rho(u\alpha' + v\beta')]}{\partial t} + \frac{\partial}{\partial x} [Q(y)\rho\alpha' + Q(y)\rho u(u\alpha' + v\beta')] \\ & + \frac{\partial}{\partial y} [Q(y)\rho\beta' + Q(y)\rho v(u\alpha' + v\beta')] \\ & - P \left[\frac{\partial \alpha' Q(y)}{\partial x} + \frac{\partial \beta' Q(y)}{\partial y} \right] \\ & - \left[\rho u Q(y) \left(u \frac{\partial \alpha'}{\partial x} + v \frac{\partial \alpha'}{\partial y} \right) + \rho v Q(y) \left(u \frac{\partial \beta'}{\partial x} + v \frac{\partial \beta'}{\partial y} \right) \right] = 0 \end{aligned}$$

$$\begin{aligned} \alpha''(6) + \beta''(7) \quad & \frac{\partial [Q(y)\rho(u\alpha'' + v\beta'')]}{\partial t} + \frac{\partial}{\partial x} [Q(y)\rho\alpha'' + Q(y)\rho u(u\alpha'' + v\beta'')] \\ & + \frac{\partial}{\partial y} [Q(y)\rho\beta'' + Q(y)\rho v(u\alpha'' + v\beta'')] \\ & - P \left[\frac{\partial \alpha'' Q(y)}{\partial x} + \frac{\partial \beta'' Q(y)}{\partial y} \right] \\ & - \left[\rho u Q(y) \left(u \frac{\partial \alpha''}{\partial x} + v \frac{\partial \alpha''}{\partial y} \right) + \rho v Q(y) \left(u \frac{\partial \beta''}{\partial x} + v \frac{\partial \beta''}{\partial y} \right) \right] = 0 \end{aligned}$$

Introducing the curvature of the co-ordinate lines and angle variations, the corresponding integral formulation is (for the complete set of equations)

$$\begin{aligned} \iint_S \rho Q(y) \sqrt{g} \, d\xi d\eta - \iint_S \rho v^n Q(y) \sqrt{g_{11}} \, d\xi dt \\ + \iint_S \rho \mu^n Q(y) \sqrt{g_{22}} \, d\eta dt = 0 \end{aligned}$$

$$\begin{aligned} \iint_S \rho \mu^k Q(y) \sqrt{g} \, d\xi d\eta - \iint_S \rho \mu^k v^n Q(y) \sqrt{g_{11}} \, d\xi dt \\ + \iint_S (\rho \beta + \rho \mu^k \mu^n) Q(y) \sqrt{g_{22}} \, d\eta dt \\ - \iiint_V P \frac{\partial}{\partial \xi} \left(\frac{\sqrt{g} Q(y)}{\sqrt{g_{11}}} \right) d\xi d\eta dt \\ - \iiint_V \rho v \left[\mu K_{\eta=cste} + v (K_{\xi=cste} + \frac{1}{\sqrt{g_{22}}} \frac{\partial [\eta, \xi]}{\partial \eta}) \right] \beta Q(y) \sqrt{g} \, d\xi d\eta dt = 0 \end{aligned}$$

$$\begin{aligned} \iint_S \rho v^k Q(y) \sqrt{g} \, d\xi d\eta - \iint_S (\rho \beta + \rho v^k v^n) Q(y) \sqrt{g_{11}} \, d\xi dt \\ + \iint_S (\rho v^k \mu^n) Q(y) \sqrt{g_{22}} \, d\eta dt \\ - \iiint_V P \frac{\partial}{\partial \eta} \left(\frac{\sqrt{g} Q(y)}{\sqrt{g_{22}}} \right) d\xi d\eta dt \\ - \iiint_V \rho \mu \left[v K_{\xi=cste} + \mu (K_{\eta=cste} - \frac{1}{\sqrt{g_{11}}} \frac{\partial [\eta, \xi]}{\partial \xi}) \right] \beta Q(y) \sqrt{g} \, d\xi d\eta dt = 0 \end{aligned}$$

$$\iint_S \rho e Q(y) \sqrt{g} d\xi d\eta - \iint_S (\rho e + p) v^n Q(y) \sqrt{g_{11}} d\xi dt + \iint_S (\rho e + p) \mu^n Q(y) \sqrt{g_{22}} d\eta dt = 0$$

c) (ξ, η) numerical scheme

The following curvilinear moving grid scheme can then be derived from the above integral equations as in the cartesian case.

$$[\rho]^\circ I^\circ - [\rho] I_\circ - \tau[\rho]_{12} \{ [v^n]_{12} - [\beta v^*]_{12} \} I_{12} + \tau[\rho]_{43} \{ [v^n]_{43} - [\beta v^*]_{43} \} I_{43} + \tau[\rho]_{23} \{ [\mu^n]_{23} - [\beta \mu^*]_{23} \} I_{23} - \tau[\rho]_{14} \{ [\mu^n]_{14} - [\beta \mu^*]_{14} \} I_{14} = 0$$

$$[\rho \mu^k]^\circ I^\circ - [\rho(\mu + \alpha v)]_\circ I_\circ - \tau[\rho \mu^k]_{12} \{ [v^n]_{12} - [\beta v^*]_{12} \} I_{12} + \tau[\rho \mu^k]_{43} \{ [v^n]_{43} - [\beta v^*]_{43} \} I_{43} + \tau[\rho(\beta \mu^n + \alpha v^k)]_{23} \{ [\mu^n]_{23} - [\beta \mu^*]_{23} \} I_{23} - \tau[\rho(\beta \mu^n + \alpha v^k)]_{14} \{ [\mu^n]_{14} - [\beta \mu^*]_{14} \} I_{14} - \tau \{ [\rho]_{14} - [\rho]_{23} \} \frac{1}{2} (\beta_{23} I_{23} + \beta_{14} I_{14}) - \tau[\rho v]_\circ \{ ([\mu]_\circ - [\mu^*]_\circ) [K_{\eta=cste}]_\circ + ([v]_\circ - [v^*]_\circ) [K_{\xi=cste} + \frac{1}{\sqrt{g_{22}}} \frac{\partial[\eta, \xi]}{\partial \eta}]_\circ \} \beta_\circ I_\circ = 0$$

$$[\rho v^k]^\circ I^\circ - [\rho(v + \alpha \mu)]_\circ I_\circ - \tau[\rho(\beta v^n + \alpha \mu^k)]_{12} \{ [v^n]_{12} - [\beta v^*]_{12} \} I_{12} + \tau[\rho(\beta v^n + \alpha \mu^k)]_{43} \{ [v^n]_{43} - [\beta v^*]_{43} \} I_{43} + \tau[\rho v^k]_{23} \{ [\mu^n]_{23} - [\beta \mu^*]_{23} \} I_{23} - \tau[\rho v^k]_{14} \{ [\mu^n]_{14} - [\beta \mu^*]_{14} \} I_{14} - \tau \{ [\rho]_{12} - [\rho]_{43} \} \frac{1}{2} (\beta_{12} I_{12} + \beta_{43} I_{43}) - \tau[\rho \mu]_\circ \{ ([\mu]_\circ - [\mu^*]_\circ) [K_{\eta=cste}]_\circ - \frac{1}{\sqrt{g_{11}}} \frac{\partial[\eta, \xi]}{\partial \xi}]_\circ + ([v]_\circ - [v^*]_\circ) [K_{\xi=cste}]_\circ \} \beta_\circ I_\circ = 0$$

$$[\rho(\epsilon + \frac{q^2}{2})]^\circ I^\circ - [\rho(\epsilon + \frac{q^2}{2})]_\circ I_\circ - \tau \{ [\rho(\epsilon + \frac{q^2}{2})]_{12} \{ [v^n]_{12} - [\beta v^*]_{12} \} + [\rho v^n]_{12} \} I_{12} + \tau \{ [\rho(\epsilon + \frac{q^2}{2})]_{43} \{ [v^n]_{43} - [\beta v^*]_{43} \} + [\rho v^n]_{43} \} I_{43} + \tau \{ [\rho(\epsilon + \frac{q^2}{2})]_{23} \{ [\mu^n]_{23} + [\beta \mu^*]_{23} \} + [\rho \mu^n]_{23} \} I_{23} - \tau \{ [\rho(\epsilon + \frac{q^2}{2})]_{14} \{ [\mu^n]_{14} - [\beta \mu^*]_{14} \} + [\rho \mu^n]_{14} \} I_{14} = 0$$

The hydrodynamic quantities appearing in the numerical fluxes are determined by the resolution of 1-D Riemann problems but the normal and tangential velocity components on one side of a cell edge take the curvature of the coordinate lines into account considering (μ^k, v^n) [resp. (v^k, μ^n)] as constants along a ξ -line [resp. η -line]. In axisymmetric geometries I_o , I^o and I_{ij} are respectively cell volumes at old and new time level and surface of the curved edge (ij) at the initial time.

2.3 - Second order accuracy extension

We are working now on a second order accuracy extension of this method.

The complete set of 2-D curvilinear moving grid hydro equations is splitted into two 1-D hyperbolic systems.

$$\frac{\partial}{\partial \tau} \psi' + A' \frac{\partial}{\partial \xi} \psi' = B'$$

$$\frac{\partial}{\partial \tau} \psi'' + A'' \frac{\partial}{\partial \eta} \psi'' = B''$$

with
$$\psi' = \begin{pmatrix} \mu_k^n \\ v^k \\ \rho \\ p \end{pmatrix}, \quad \psi'' = \begin{pmatrix} v_k^n \\ \mu^k \\ \rho \\ p \end{pmatrix}$$

Roe's general second order method /8, 10/ is then applied to each system.

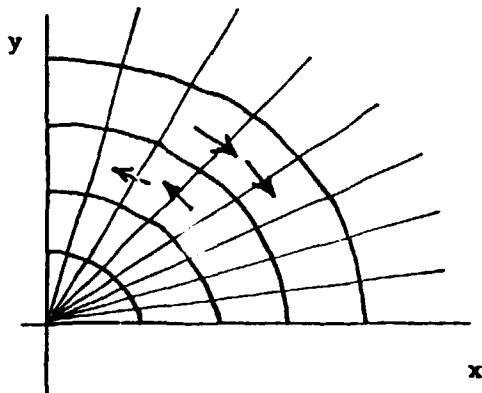
3. - GRID GENERATION ALGORITHMS

Any grid motion that satisfies the stability condition of the explicit moving grid scheme can be used in a GAIA computation.

A simple algorithm is particularly well suited for quasi 1-D cylindrical and spherical problems. The grid points are assumed to move in the most lagrangian way along fixed angular directions. This is done by solving the radial Riemann problems of the 2-D grid, then interpolating the resulting fluid velocities at the grid points and finally moving these grid points along the fixed direction at the

correct apparent velocity. The complete formula using the curvature of the cell edges are not reported here.

Such a grid motion behaves as lagrangian in the radial direction, as eulerian in the transverse direction. Since the discontinuities of tangential velocity are disregarded interfacial slips are taken into account without particular care.



4. - NUMERICAL RESULTS

- (a) The first exemple fig. 1 is the shock tube problem used by Sod /7/. The tube extends from $x = 0$ to $x = 1$ and is divided into 100 equal cells. A perfect gas is initially at rest with $p = 1$, $\rho = 1$ for $0 \leq x < .5$, $p = .1$, $\rho = 0.125$ for $0.5 < x < 1$ with $\gamma = 1.4$.

The problem is run with lagrangian and eulerian grids using the second order scheme. Reduced diffusion appears in both lagrangian and eulerian limits.

- (b) The second exemple fig. 2 illustrates the convergence of the Godunov method when used in reactive flow.

The stationnary reaction zone of a plane 1-D detonation wave is solved using equation of state (2) for the mixture of condensed and gaseous components. One can check the good agreement with the Z.N.D model. The numerical points are well aligned along the Rayleigh line between the C.J state and the von Neumann spike. The pressure-burn fraction profile is also in agreement with the EOS dependent theoretical solution.

- (c) The 2-D abilities of the GAIA code are illustrated fig.3 by the computation of a hypersonic flow around a compressible sphere. Such a calculation was first presented by Noh /2/ with the Coupled Eulerian-Lagrangian code.

An unique computational domain is now considered. Very important slip is noticeable on the flow velocity diagrams. However, no particular smoothing is applied to the interfaces and the logical grid connectivity is maintained during the whole calculation.

CONCLUSIONS

Designed for applied physics problems, the GAIA hydrodynamic computer code offers specific advantages over its Lagrangian, Coupled Eulerian-Lagrangian or Arbitrary Lagrangian-Eulerian counterparts /2, 3, 5, 11/.

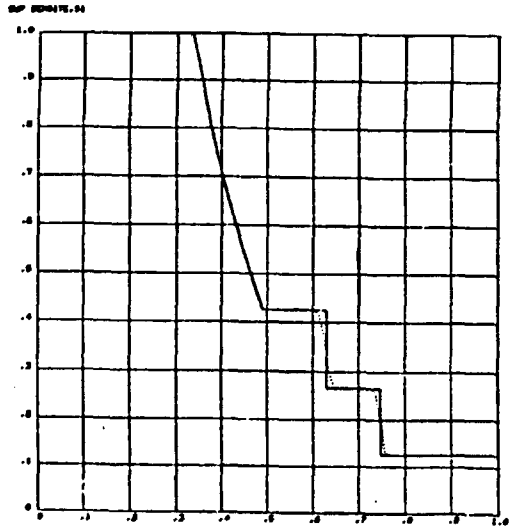
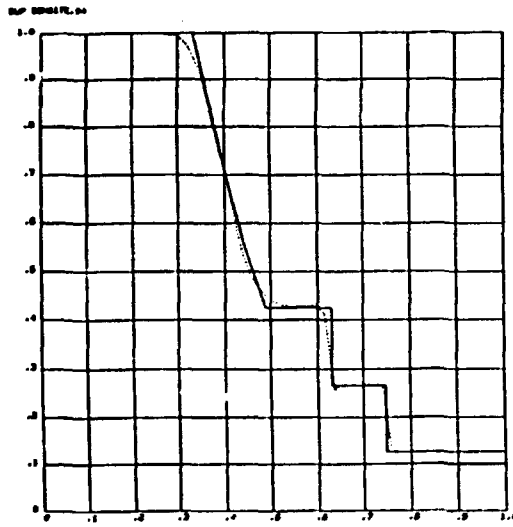
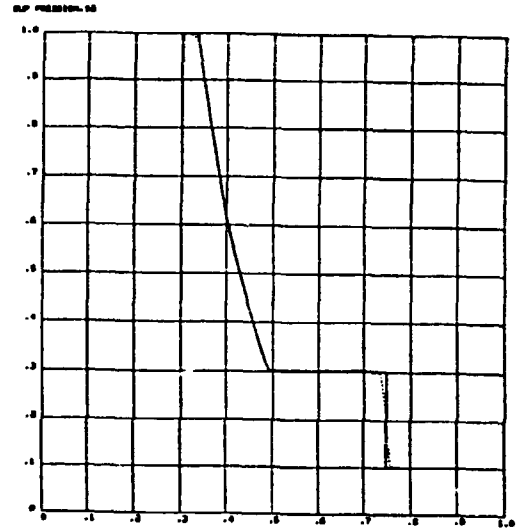
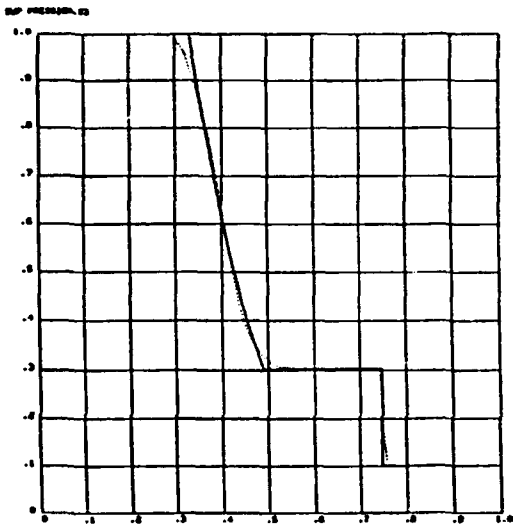
Thanks to curvilinear coordinates, it allows cheap computations of quasi 1-D flows requiring few grid points in the transverse direction.

In trully 2-D flows :

- shocks are well resolved especially at the interfaces,
- the moving grid scheme allows continuous rezone without excessive numerical diffusion, a dramatic contribution to the overall code robustness,
- slip lines can be handled without specific treatment using a simple connected grid.

REFERENCES

1. - S.K. GODUNOV and all, Zh. Vycisl. Mat. Fiz. 1,1020 (1961)
2. - W.F. NOH in "Methods in Computational Physics", Academic Press (1964)
3. - M.L. WILKINS in "Methods in Computational Physics", Academic Press (1964)
4. - F.H. HARLOW and A.A. AMSDEN, "Fluid Dynamics", LA-4700, Los Alamos, New Mexico (1971)
5. - C.W. HIRT, A.A. AMSDEN and J.L. COOK, J. Comput. Phys. 14,227-253 (1974)
6. - S.K. GODUNOV, A.W. ZABRODIN and ail, "Numerical Solution of Multidimensional Gas Dynamics Problems", Nauka, Moscow (1976)
7. - G.A. SOD, J. Comput. Phys. 27 (1978), 1
8. - P.L. ROE, J. Comput. Phys. 43 (1981), 357
9. - J.K. DUKOWICZ, J. Comput. Phys. 61 (1985), 119
- 10.- P.L. ROE, Ann. Rev. Fluid Mech. 18 (1986), 337
- 11.- F.L. ADESSIO and all, "CAVEAT : A Computer Code for Fluid Dynamics Problems with Large Distorsion and Internal Slip", LA-10613-MS, Los Alamos, New Mexico (1986)



LANGRANGIAN : MIN-MOD LIMITER

EULERIAN : SUPERBEE LIMITER

HYDRODYNAMIQUE GATA

BETONIQUE
1-3

..... D'EXPLOSER FICTIF
PUN=500 KGMS. PCJ=200 KGMS

ROZENO = 1.844 (G/CM3)
DCJ = 8900 (R/S)
GAPRACJ = 2.91

PAILLAGE: 4. COUCHES/CM
C.P.L. 1.0

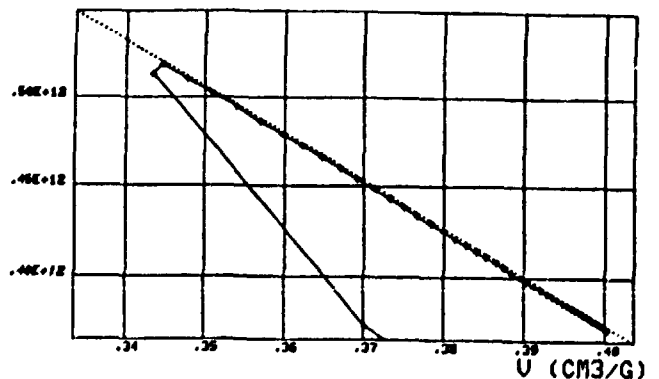
RESOLUTION
ZONE DE REACTION
STATIONNAIRE

FIGURE 2

LARS=	.000	PRAT=.20E+07	U=-.41E+01
LARS=	.000	PRAT=.45E+09	U=-.99E+03
LARS=	.012	PRAT=.53E+11	U=-.85E+05
LARS=	.151	PRAT=.37E+12	U=-.25E+06
LARS=	.261	PRAT=.51E+12	U=-.32E+06
LARS=	.361	PRAT=.52E+12	U=-.32E+06
LARS=	.442	PRAT=.51E+12	U=-.31E+06
LARS=	.521	PRAT=.54E+12	U=-.31E+06
LARS=	.584	PRAT=.49E+12	U=-.30E+06
LARS=	.620	PRAT=.49E+12	U=-.30E+06
LARS=	.626	PRAT=.49E+12	U=-.30E+06
LARS=	.626	PRAT=.49E+12	U=-.30E+06
LARS=	.725	PRAT=.47E+12	U=-.29E+06
LARS=	.762	PRAT=.47E+12	U=-.29E+06
LARS=	.792	PRAT=.46E+12	U=-.29E+06
LARS=	.810	PRAT=.45E+12	U=-.28E+06
LARS=	.841	PRAT=.45E+12	U=-.28E+06
LARS=	.861	PRAT=.44E+12	U=-.27E+06
LARS=	.874	PRAT=.44E+12	U=-.27E+06
LARS=	.894	PRAT=.42E+12	U=-.27E+06
LARS=	.907	PRAT=.42E+12	U=-.27E+06
LARS=	.910	PRAT=.42E+12	U=-.27E+06
LARS=	.920	PRAT=.42E+12	U=-.27E+06
LARS=	.920	PRAT=.42E+12	U=-.27E+06
LARS=	.945	PRAT=.41E+12	U=-.26E+06
LARS=	.952	PRAT=.41E+12	U=-.26E+06

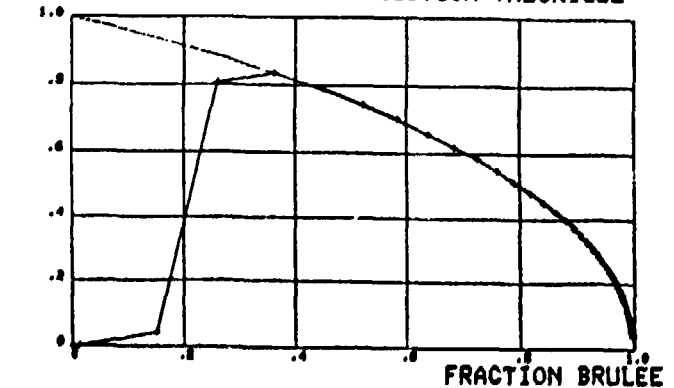
PRESSON (CGS)

— DROITE DE RAYLEIGH



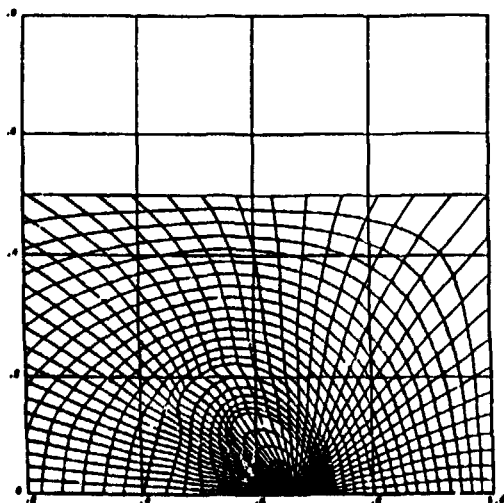
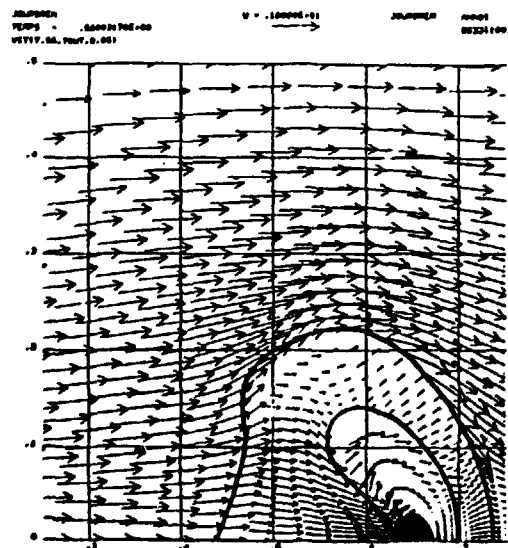
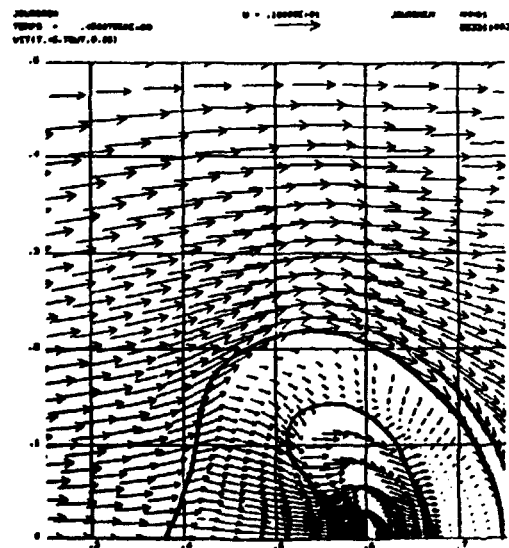
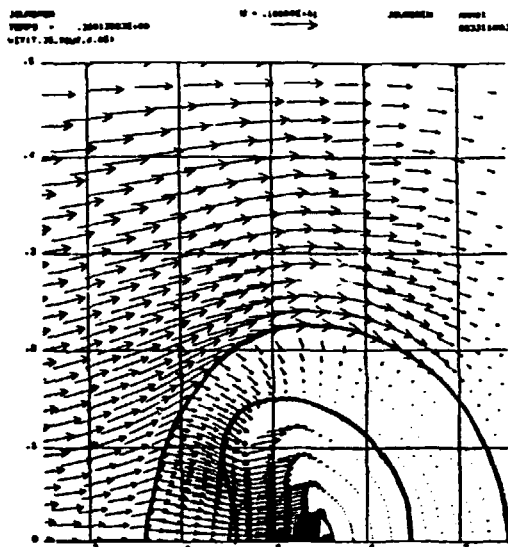
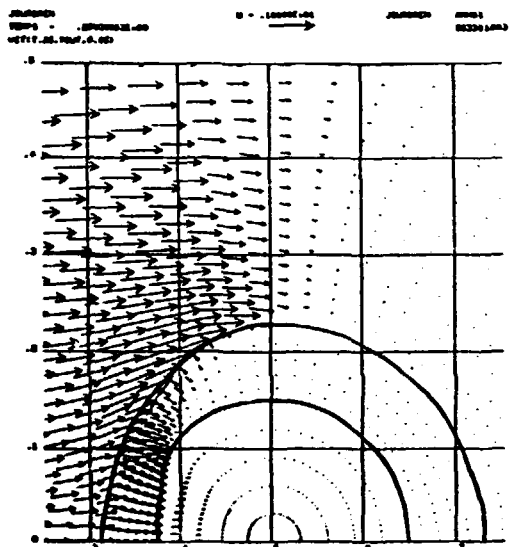
(P-PCJ)/(PUN-PCJ)

— SOLUTION THEORIQUE



FRACTION BRULEE

FIGURE 3



FINAL TIME GRID